Available online at www.sciencedirect.com
ScienceDirect
Agricultural and Forest Meteorology 138 (2006) 93–103
AGRICULTURAL AND FOREST METEOROLOGY
www.elsevier.com/locate/agrformet

Contrasting mean vertical motion from tilt correction methods and mass continuity

Dean Vickers *, L. Mahrt

College of Oceanic and Atmospheric Sciences, COAS Admin Bldg 104, Oregon State University, Corvallis, OR 97331-5503, USA

Received 15 December 2005; accepted 5 April 2006

Abstract

Mean vertical motion is computed from 3D sonic anemometer measurements using three different tilt correction methods. The mean vertical motion is sensitive to the choice of tilt correction method. For a given tilt correction approach, the mean vertical motion is sensitive to the time-scale chosen for averaging the wind components.

The mean vertical motion is also computed from mass continuity using the horizontal divergence estimated from a network of 2D sonic anemometers. The estimate based on mass continuity is more in agreement with the subsidence expected from the decrease of roughness in the downwind direction at the site. Because all the tilt correction methods assume that the long-term mean vertical motion is zero, albeit in different forms, they fail to reproduce the vertical motion based on the persistent horizontal divergence. The mean vertical motion from the mass continuity equation has much less scatter compared to that based on the 3D sonic anemometer. However, the magnitude of the divergence can be dependent on the spatial scale over which the horizontal gradients are calculated.

The eddy flux, storage and advection terms in the budget equation for net ecosystem exchange of carbon are evaluated. Estimates of advection of carbon dioxide based on mass continuity are more plausible than estimates based on the tilt correction methods.

Keywords: Advection; Mean vertical motion; Tilt correction; Horizontal divergence

1. Motivation

Early studies estimating net ecosystem exchange of carbon (NEE) typically included only the eddy flux and storage components. This method often leads to an underestimate of the expected nocturnal respiration of carbon dioxide on nights with weak mixing. One possible interpretation of the missing carbon dioxide is that horizontal and vertical advection are important (Lee, 1998; Baldocchi et al., 2000; Aubinet et al., 2003; Staebler and Fitzjarrald, 2004; Aubinet et al., 2005). An empirical ''patch'' for this problem is the u_*-filter approach, where the measured eddy flux plus storage during weak turbulence periods is replaced with a model of the respiration based on the eddy flux plus storage during strong mixing nocturnal periods (e.g., Goulden et al., 1996; Falge et al., 2001; Pattey et al., 2002).

The method of calculating NEE proposed by Lee (1998) added the vertical advection term to the storage and eddy flux terms in the NEE budget. This approach was applied by Baldocchi et al. (2000) who reported that including vertical advection improved their budget closure, however, they inferred that horizontal advection may also be important. Aubinet et al. (2003) concluded that horizontal advection of carbon dioxide was mostly cancelled by vertical advection. Their hypothesis was that horizontal and vertical advection are linked by an entrainment mechanism where the air above the canopy

* Corresponding author.
E-mail address: vickers@coas.oregonstate.edu (D. Vickers).

0168-1923/$ – see front matter
doi:10.1016/j.agrformet.2006.04.001

is mixed downward into the subcanopy drainage flow. This suggests that it is inappropriate to include only the vertical component of advection in the budget (Finnigan, 1999). Staebler and Fitzjarrald (2004) found that vertical advection of carbon dioxide was small while horizontal advection was significant. Feigenwinter et al. (2004) found that horizontal and vertical advection of carbon dioxide tended to cancel at night, yet pointed out that the large scatter in the advective fluxes needs further investigation. Aubinet et al. (2005) raised the question of the sensitivity of the vertical motion estimate to small errors in the tilt correction procedures and suggested that future work use the mass conservation equation. They suggested that measuring the divergence could be a more robust approach compared to measuring the vertical velocity at a single point.

All of the above studies estimate mean vertical motion by applying a tilt correction to the vertical velocity measured by a 3D sonic anemometer, however, it has not been demonstrated that such an approach is adequate for estimating mean vertical motion. Can the true vertical motion be extracted from the measurements which are contaminated by flow distortion, tilt of the sensor and variable sloping terrain? In this study, we investigate the feasibility of quantifying mean vertical motion and vertical advection of CO_2 using sonic anemometer measurements.

A network of towers was deployed to provide two independent estimates of mean vertical motion: (1) from measurement of vertical velocity at a central tower and a tilt correction, and (2) from measurement of the horizontal divergence using a network of towers surrounding the central tower. From incompressible mass continuity, the time-averaged vertical velocity based on the divergence is given by

$$\bar{w}(h) = -\int_{z=0}^{z=h} \left(\frac{\partial \bar{u}}{\partial x} + \frac{\partial \bar{v}}{\partial y} \right) \mathrm{d}z \qquad (1)$$

where the overbars denote a time-average.

The field measurement site is described in Section 2. The tilt correction methods are compared in Section 3, and the mass continuity method is presented in Section 4. The different estimates of $\bar{w}$ are contrasted in Section 5 and analysis of the NEE budget including advection terms is presented in Section 6. Conclusions follow in Section 7.

2. Field experiment

The primary measurements were taken during the dry season at a semi-arid ponderosa pine site in central Oregon, U.S.A. at 1008 m elevation during August, September and October of 2004. The site consists of a very homogeneous stand of 3-m tall, 18 year old pine trees in a region of size 300 m × 275 m (Fig. 1). Within the boundary, the average leaf area index is 0.52 and the tree density is 370 trees per ha. The site location is 44 18 56N, 121 36 28W.

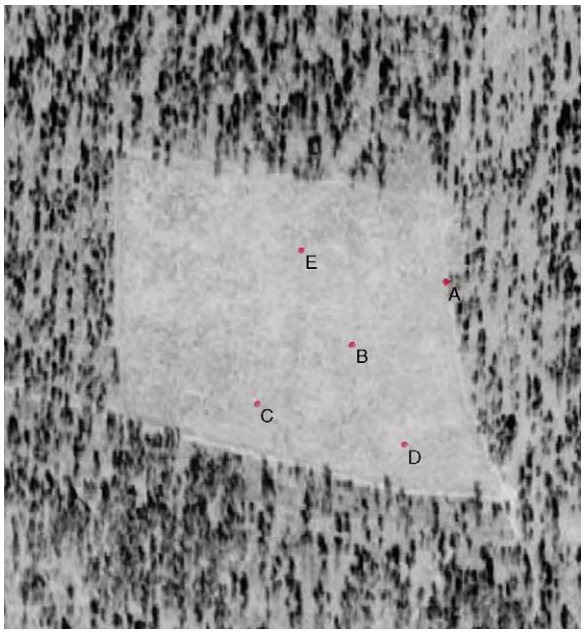

Fig. 1. Overhead view of the young pine site with the 2004 field program towers A–E. The region with young pines appears gray and the surrounding region with taller, older pines appears as gray with black streaks. The dimensions of the region of young pines is approximately 300 m × 275 m. A network of four inner towers (not shown) were added half way between the central tower B and the other four existing towers in the 2005 sensitivity study of the scale-dependence of the divergence.

The area within the site boundary was clear cut and replanted as an experimental research site by the U.S. Forest Service in 1987. A heterogeneous stand of older and taller pines surround the site on all sides. The sparse trees surrounding the site range in height from 5 to 30 m and in age from 20 to 100 years. The site was chosen in part due to the large roughness change and the expected acceleration of the mean flow (divergence and subsidence) over the shorter trees.

The terrain slopes upward to the southwest and west with 100 m elevation gain over 5 km, or a slope of about 2%, and slopes weakly downward ($< 1\%$) or is flat in other directions. More than one-half the time the wind direction was in the sector 230°–300° (from the west). The site is characterized by sustained synoptic high pressure and weak large-scale flow in summer and fall. For the 3-month experiment, the average wind

speed was 0.7, 1.4 and 1.9 m s^{-1} at the 1, 5 and 12-m levels on tower B, respectively.

The central tower was equipped with 3D CSAT3 sonic anemometers (Campbell Scientific Inc.) at 5 and 12 m above ground recording the three wind components and the sonic temperature at 10 Hz. 2D sonic anemometers (Vaisala Inc., formerly Handar) were deployed at 1, 5 and 12 m above ground on towers A and C and at 1 and 5 m on towers D, E and B for measuring the mean horizontal wind. All periods with flow in the sector 60°–150° were discarded because of possible flow distortion due to flow through the tower and support structures prior to reaching the CSAT3 anemometers.

3. Tilt correction

3.1. Background

A tilt correction is normally applied to 3D sonic anemometer wind measurements to remove: (1) influence of flow distortion, (2) apparent vertical motion due to tilt of the sensor from true (gravitational) vertical, and (3) apparent vertical motion due to sloping topography. These influences lead to an artificial wind direction dependence of the vertical velocity as measured by the anemometer. As noted by Paw U et al. (2000) and others, it is not possible to distinguish between these effects from the vertical velocity measurements alone. Directionally dependent flow distortion effects are sometimes assumed to be accounted for by the internal software in the anemometer, although Högström and Smedman (2004) recently pointed out that the manufacturer's corrections, which are based on relatively weak turbulence wind tunnel studies, may not be optimum for the stronger turbulence conditions found in the field. Prior to any tilt correction approach, a zero wind calibration should be performed on the anemometer to remove any potential offsets.

Historically, many investigators have rotated the three wind components into streamline coordinates for each 30-min or 1-h time period (e.g., Kaimal and Finnigan, 1994). This approach defines the short-term mean vertical motion to be zero. The main motivation for this approach was that the mean vertical motion measurements could not be trusted due to contamination by sensor tilt, elevation slope, limited sample size and flow distortion. More recently, Lee (1998) and others identified the importance of non-zero $\bar{w}$ for calculating vertical advection of carbon dioxide. Even very small values of $\bar{w}$ can lead to significant advection in the presence of large vertical gradients, such as typically found for CO_2 near the surface on nights with weak mixing. Since the streamline coordinates approach exactly removes all short-term mean vertical motion, other methods were adopted which allow non-zero short-term $\bar{w}$.

Commonly, the long-term $\bar{w}_m(\phi)$ averaged over weeks to months is removed from the short-term averages of $\bar{w}_m$, where ϕ is wind direction and $\bar{w}_m$ is the measured time-averaged vertical velocity (Lee, 1998; Baldocchi et al., 2000; Paw U et al., 2000; Wilzcak et al., 2001; Finnigan et al., 2003). This approach assumes that the long-term mean vertical motion for a given wind direction is zero. The short-term deviations in $\bar{w}$ that remain after removing the long-term $\bar{w}_m(\phi)$ are presumed to correspond to real events. Long-term measurements, without disturbing the anemometer and the flow distortion environment, are required to implement this approach in order to obtain robust estimates of $\bar{w}_m(\phi)$.

While the philosophy of removing the directionally dependent, long-term mean vertical motion is present in most current tilt correction methods, the details of application vary. Lee (1998) proposed linear regression of $\bar{w}_m$ on the mean horizontal wind speed separately for each wind direction category, which accounts for the fact that the apparent vertical motion due to sensor tilt is proportional to the horizontal wind speed. In the planar fit technique (Wilczak et al., 2001), multiple linear regression of $\bar{w}_m$ on the two horizontal wind components results in a tilted plane. This method applies to the idealized case where the surface is uniformly tilted (planar) with respect to the sensor, or equivalently, where the sensor is tilted over perfectly flat terrain.

A third more general approach examines the wind direction dependence of the tilt angle (Paw U et al., 2000; Vickers and Mahrt, 2003; Feigenwinter et al., 2004). When the ϕ-dependence of the tilt angle can be approximated by a simple sinusoidal function of azimuth angle, this method is identical conceptually to the planar fit technique. In this sense, the planar fit approach is a special case of the tilt angle method. For non-idealized terrain, a planar fit may not be appropriate, and an incremental bin-average representation of the tilt angle dependence on ϕ may be more suitable.

The regression used by Lee's approach and the planar fit method exactly remove the mean vertical motion averaged over the entire experiment, while the tilt angle method does not. Lee's approach removes the long-term $\bar{w}$ for each wind direction category individually, while the planar fit and tilt angle methods do not.

3.2. Problems

As pointed out by Lee (1998), a potential problem is that the tilt correction approach may remove real vertical motion associated with local circulations driven by surface heterogeneity. Examples include a change in surface roughness, differential daytime heating and systematic diverging (or converging) nocturnal drainage flows. The flow in this study is influenced by a surface roughness change. It is not known if systematic circulations induced by daytime differential heating are important. For westerly flow, the site is approximately at the bottom of a slope, although the slope is weak, and it is not known if the drainage flow is accelerating or decelerating at the site. A complication with identifying the drainage flow is that the predominant weak large-scale flow is from the same direction as the drainage flow.

Given the rough-to-smooth surface roughness change for all wind directions, and the persistent synoptic high pressure pattern during our field program, we would expect overall mean sinking motion at the site. Such long-term mean vertical motion would be at least partially removed by any of the tilt correction methods described above.

3.3. Application

The same procedures are applied independently to the 5 and 12-m levels. We focus on 12 m because the signal-to-noise ratio in $\bar{w}$ should increase with height above the surface, the 5-m measurements are more likely to be contaminated by individual roughness elements (3-m trees) and therefore be less representative of the spatial area over which the divergence is measured, and because we are interested in computing the vertical advection of CO_2 through the 12-m level where the eddy-correlation CO_2 flux is measured.

Averaging times for application of the tilt correction vary substantially in the literature. For example, Berger et al. (2001) use 1-h average wind components and Wilczak et al. (2001) propose using 5-min averages to derive the regression coefficients in the planar fit approach. Longer averaging times resolve less wind direction variability while shorter averaging times become impractical at some point for the planar fit method where a matrix must be inverted to perform the multiple regression. All time mean quantities in this section, denoted with an overbar, represent 100-s time averages. The sensitivity of the tilt angle method to averaging time is discussed in Section 3.5.

The Lee (1998) approach regresses the vertical velocity on the horizontal wind speed for each wind direction category, generating a sequence of wind direction dependent coefficients $\alpha(\phi)$ and $\beta(\phi)$. The corrected mean vertical velocity ($\bar{w}$) is then given by

$$\bar{w} = \bar{w}_{\mathrm{m}} - (\alpha(\phi) + \beta(\phi)U) \tag{2}$$

where we use 36 wind direction categories of width 10° each and the mean horizontal wind speed is given by

$$U = (\bar{u}^2 + \bar{v}^2)^{1/2}. \tag{3}$$

The planar fit approach uses multiple regression of the vertical velocity on the two components of the horizontal wind, and the corrected vertical motion is given by

$$\bar{w} = \bar{w}_{\mathrm{m}} - (a + b\bar{u} + c\bar{v}) \tag{4}$$

where the single-valued coefficients a, b and c are calculated using all the data. The tilt angle approach calculates a tilt angle as

$$T_{\mathrm{a}} = \arctan\left(\frac{\bar{w}_{\mathrm{m}}}{U}\right). \tag{5}$$

Here we temporarily remove periods with the weakest mean flow ($U < 0.5$ m s^{-1}), where calculation of the tilt angle is not well posed and the tilt angle becomes erratic (e.g., Paw U et al., 2000). The corrected mean vertical velocity is then estimated for all the data, including the weakest wind periods, as

$$\bar{w} = \bar{w}_{\mathrm{m}} - U\tan\left(T_{\mathrm{a}}(\phi)\right) \tag{6}$$

where $T_{\mathrm{a}}(\phi)$ is the bin-averaged wind direction dependent tilt angle using 36 wind direction categories.

3.4. Comparison of tilt correction methods

The three different tilt correction methods yield three different estimates of $\bar{w}$ (Fig. 2). While the correlations between 30-min average $\bar{w}$ estimates are high, the root-mean-square differences of a few cm s^{-1} are significant, and the maximum differences are as large as 10 cm s^{-1}. These large differences are discouraging for prospects of estimating mean vertical motion using a tilt correction because the estimate of $\bar{w}$ is sensitive to the details of the approach used and it is difficult to identify an obviously superior method. The magnitude of the tilt angles found here (Fig. 3) are comparable to, or smaller than, what we have typically found for other sites on relatively flat terrain with carefully leveled anemometers.

Differences between the bin-averaged $T_{\mathrm{a}}(\phi)$ values and a pure sinusoidal dependence, as implied by the planar fit method, may be partially due to an insufficient number of samples (random sampling error) for the less

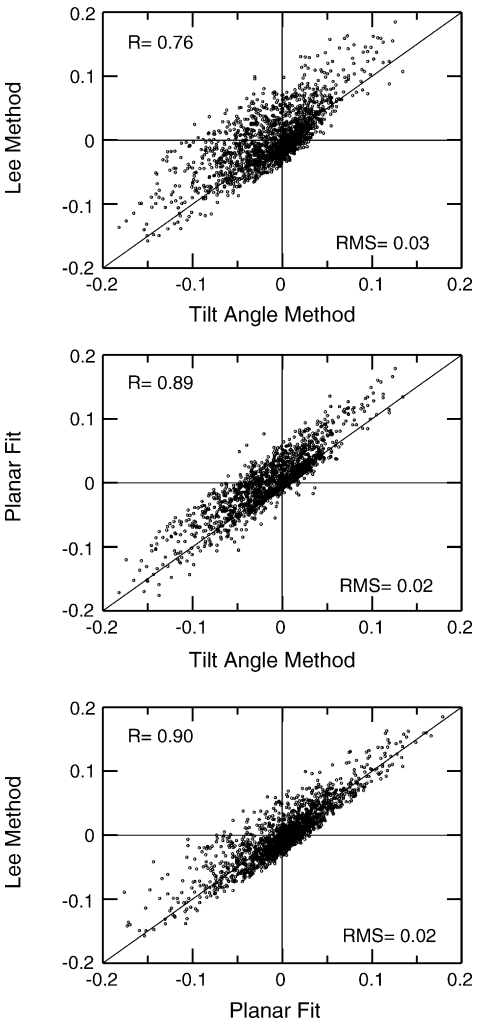

Fig. 2. Comparison of 30-min mean vertical motion (m s^{-1}) at 12 m for three different tilt correction methods.

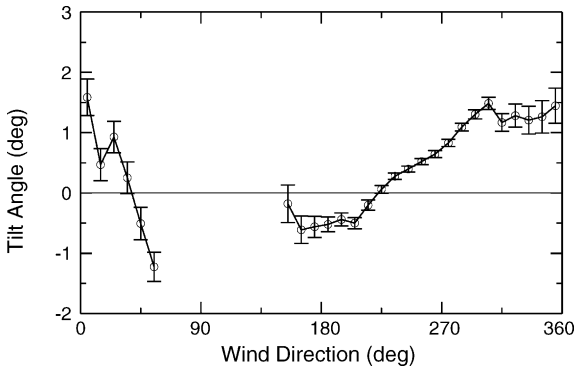

Fig. 3. Mean and standard error of the tilt angle as a function of wind direction (100-s average data at 12 m).

frequent wind directions. On the other hand, the site may be characterized by directionally dependent slopes that cannot be reasonably represented by a planar fit, in which case the bin-averages of $T_a(\phi)$ are the better representation. In addition, higher-order flow distortion effects may contribute to more complex azimuthal dependencies of the tilt angle, such as a double peak, which cannot be represented by the planar fit. For example, Högström and Smedman (2004) highlight the calibration problems and flow distortion characteristics of Gill Solent (R2 and R3) sonic anemometers. Such problems may be less severe for the less-obstructed design of the Campbell CSAT3.

3.5. Dependence on averaging time

An example of the sensitivity to choice of averaging time is demonstrated in Fig. 4, where only winds from the sector between 290° and 310° are included. For this narrow sector, the average tilt angle is a local maximum and does not vary significantly with wind direction. This wind sector also represents a significant percentage of the entire dataset and therefore more robust statistics.

For weak winds, 5-, 10- and 30-min averaging of the wind components lead to a tilt angle that is about 50% smaller compared to 100-s averaging. This is because longer averaging times smear out the details of the wind direction dependence, especially for weak winds. Because the tilt angle is a local maximum for the 290°–310° wind sector, short-term variations in wind direction outside the sector during the averaging period reduce the average tilt angle. For stronger and less variable winds, this effect is reduced and all four averaging times lead to nearly the same average tilt angle.

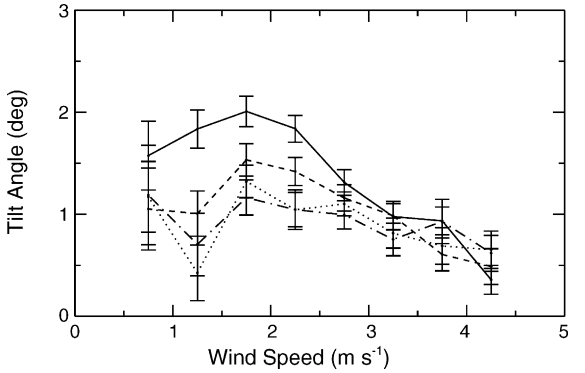

Fig. 4. Mean and standard error of tilt angle as a function of wind speed for wind directions between 290° and 310° (12 m data) for 100-s (solid), 5-min (dash), 10-min (dot) and 30-min (dash-dot) averaging of the wind components.

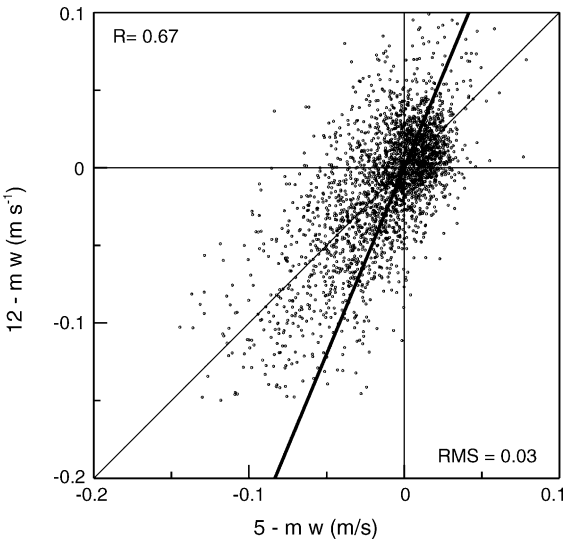

Fig. 5. Comparison of 30-min mean vertical motion at the 12-m and 5-m levels using the tilt angle method (dots). The heavy line represents the theoretical slope (12/5) one would expect if the divergence were constant with height.

A separate issue for the current dataset is that the tilt angle calculated using 100-s averaging is a function of wind speed (Fig. 4). If a tilted anemometer or sloped terrain were the only process acting, one would expect the average tilt angle to be independent of wind speed. Because we do not observe this, it may indicate a real wind speed-dependent vertical motion.

3.6. Height dependence

The $\bar{w}$ estimates from the two 3D sonic anemometers on the central tower and the tilt angle method are only weakly correlated (Fig. 5). The slope based on regression of $\bar{w}$ for the two levels is near unity, indicating that the divergence vanishes above 5 m. In light of the measured divergence (subsequent Sections), this casts doubt on the validity of $\bar{w}$ estimates from the 3D sonic anemometer and the tilt correction method. In addition, the 5-m level is presumably within the roughness sublayer and may be influenced by nearby individual roughness elements differently than the 12 m measurements.

4. Divergence estimate

No significant wind speed bias problems were found by an intercomparison study of the Handar anemometers used to measure the horizontal gradients of the mean flow. The good agreement between the 2D sonic anemometers was first documented by an intercomparison field program conducted prior to the current study. Four model 425A 2D sonic anemometers from Vaisala Inc. (formerly Handar) were deployed for intercomparison field experiments during the summers of 2000 and 2001 in a homogeneous commercial rye grass field located southeast of Corvallis, Oregon U.S.A. The differences in the mean wind from the four sonic anemometers were less than the manufacturer's wind speed accuracy specification of 3%. Due to the design of the sonic body and the transducer arms, there is no preferred wind direction sector from a flow distortion standpoint for the 2D sonics.

For calculating the divergence, the horizontal coordinate system was rotated for each 100-s period such that horizontal $\bar{u}$ gradients were proportional to $\bar{u}$ at tower A minus $\bar{u}$ at tower C, and $\bar{v}$ gradients by $\bar{v}$ at tower E minus $\bar{v}$ at tower D. The divergence is not sensitive to a 2D coordinate rotation. The horizontal gradients of $\bar{u}$ and $\bar{v}$ were calculated at the three measurement levels (1, 5 and 12 m) using finite differencing over a distance of 200 m. Vertical integration of the horizontal gradients from the surface to 12 m was performed using a piecewise linear fit to the four levels, where the horizontal gradients are assumed to vanish at the surface where the wind speed vanishes.

For the shorter towers D and E, where the measurements are limited to 1 and 5 m, we assume the horizontal gradient of the mean wind is constant with height between 5 and 12 m. The measured gradients on the taller towers support this assumption (Fig. 6). The fact that the horizontal gradient of the mean wind does not significantly change above 5 m suggests that the primary mechanism driving the divergence at this site is the surface roughness change.

The divergence calculations indicate mean sinking motion for all wind directions and all times of day and

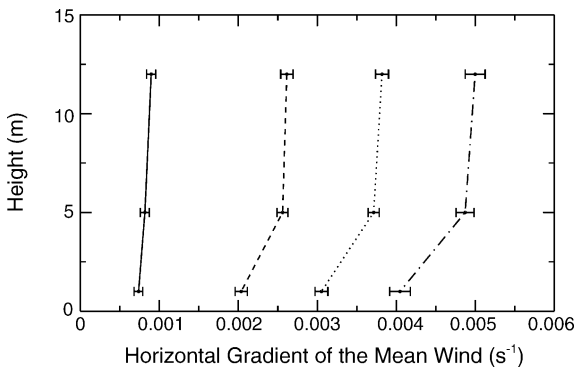

Fig. 6. Height dependence of the 30-min mean $\partial u/\partial x$ for different wind speed classes: 1–2 (solid), 2–3 (dash), 3–4 (dot), and 4–5 m s^{-1} (dash-dot).

night averaged over the 3-month experiment. We would expect to see weaker divergence due to the surface roughness change for those wind directions with longer fetch over the clearing prior to reaching the tower network. Theoretically, the divergence is a maximum at the upwind edge of the clearing and decreases with increasing distance (e.g., Garratt, 1990). The observations do indeed show that the minimum divergence occurs with north-west flow, where the tower network is located in the south-east corner of the clearing.

4.1. Sensitivity to spatial scale

An intensive field experiment was conducted in summer of 2005 (9 July– 8 August) at the same site to assess the sensitivity of the divergence to spatial scale. An inner grid of four new towers with 2D anemometers at 1 and 5 m above ground were deployed half way between the central tower and the four existing towers (Fig. 1). The inner ($\delta x = 100$ m) and outer ($\delta x = 200$ m) grids allow direct comparison of two divergence estimates where everything is held constant except the spatial scale for calculating the gradients of the mean wind.

The magnitude of the $\bar{w}$ estimates based on the inner grid are approximately a factor of two smaller than those based on the outer grid during stronger wind speed daytime conditions. The inner and outer grids yield more similar $\bar{w}$ estimates for weaker wind speed nocturnal periods. The stronger divergence for the larger grid size is consistent with stronger horizontal gradients closer to the upwind boundary (Garratt, 1990). The hypothesis is that the smaller grid misses more of the upstream region within the clearing where the divergence is larger. More detailed comparisons with internal boundary-layer theory predictions (Garratt, 1990) are not possible without detailed observations of the conditions upstream from the surface roughness change. This study indicates that, at least for this situation, the divergence is sensitive to spatial scale.

5. Direct and mass continuity methods

In this section we compare the estimates from the different tilt correction methods (the direct methods) with the $\bar{w}$ estimate based on mass continuity. All of the direct estimates of $\bar{w}$ are poorly correlated with the estimate of $\bar{w}$ based on mass continuity (Fig. 7). The standard deviation of the direct method $\bar{w}$ estimates is typically a factor of 2 greater than the standard deviation of $\bar{w}$ based on mass continuity. The correlations between $\bar{w}$ from the tilt angle method and mass continuity, and from the planar fit method and

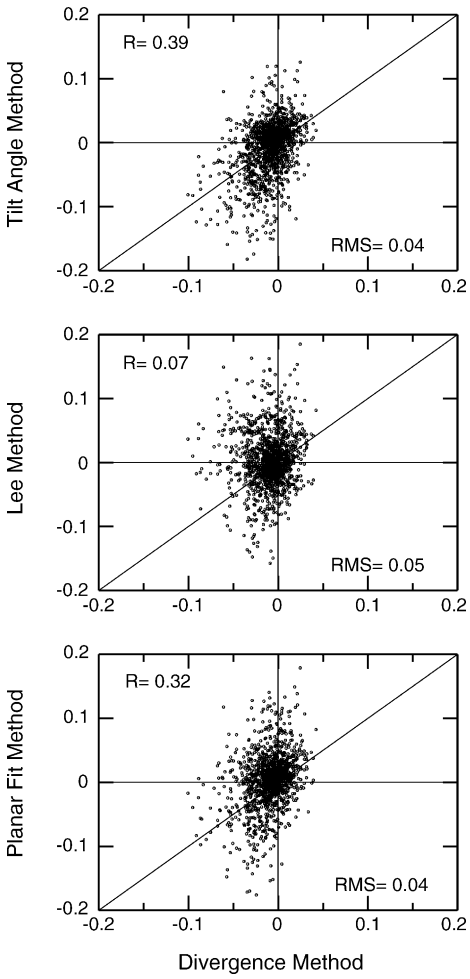

Fig. 7. 30-min mean vertical motion (m s^{-1}) at 12 m for the tilt angle, Lee, and planar fit methods as a function of the estimate based on mass continuity.

mass continuity increase with increasing averaging time, however, this is not the case for Lee's method (Fig. 8, top panel). This might imply a systematic problem with Lee's method for these data. The RMS $\bar{w}$ differences between the direct methods and the mass continuity method decrease with increasing averaging time, implying that a portion of the disagreement between the direct and mass continuity methods may be random (Fig. 8, bottom panel).

The 30-min mean vertical motion from the direct methods often exceeds 10 cm s^{-1}, which implies an increase in the mean wind speed across the 200 m network of about 1.7 m s^{-1}. Mean vertical motion of this magnitude is not supported by the divergence measurements. If a 10 cm s^{-1} $\bar{w}$ was due to an error in specification of the tilt angle, the error in the ϕ-dependence of T_a would need to be about 3° for a mean

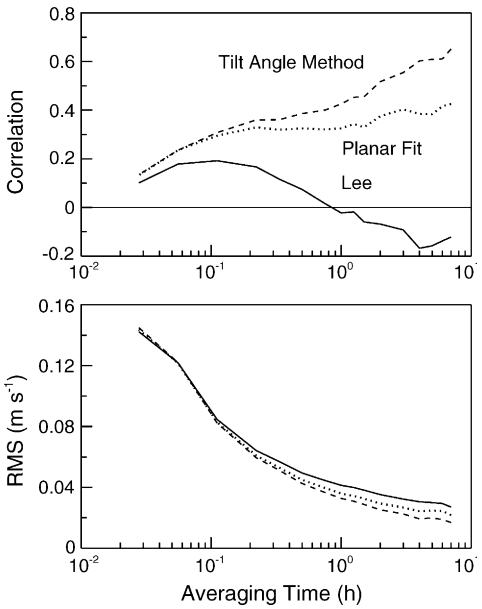

Fig. 8. Averaging time dependence of the correlation and root-mean-square error for contrasting the three direct methods with mass continuity.

wind speed of 2 m s^{-1}. It appears unlikely than an error of this magnitude occurs.

Despite the apparent noise in the direct estimates, short-term fluctuations in $\bar{w}$ from the tilt angle and mass continuity methods can be highly correlated for limited periods (Fig. 9). In this example, both the direct and mass continuity estimates clearly show sinking motion associated with stronger wind speeds, and rising motion with weaker winds. This time dependence is consistent with vertical advection of weaker horizontal momentum by rising motion and vice versa. The larger amplitude response of the direct method $\bar{w}$ compared to the mass continuity estimate for this example remains unexplained.

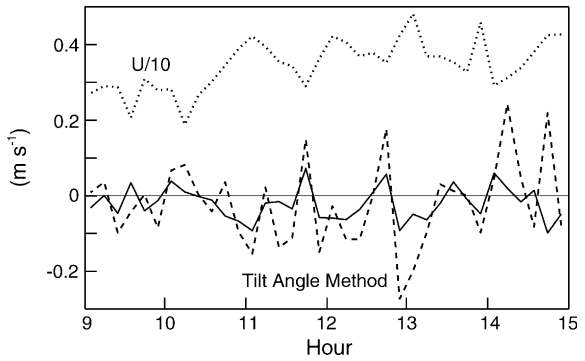

Fig. 9. Example time series of 10-min mean wind speed (divided by 10, dotted), $\bar{w}$ from tilt angle method (dashed), and $\bar{w}$ from mass continuity (solid).

5.1. Sensitivity studies

The agreement between the direct and mass continuity methods degrades further when the magnitude of $\bar{w}$ from the direct methods does not increase monotonically with height between the surface, 5 and 12 m. Such periods may represent complex flow situations that are impossible to resolve without a much finer vertical and horizontal grid of measurements. A non-monotonic increase of $\bar{w}$ with height occurred nearly one-half the time, independent of the tilt correction method. Removing such periods modestly improved the correlation between the 30-min mean $\bar{w}$ estimates from the tilt angle and mass continuity methods from 0.39 to 0.47 but large disagreement remains.

We compared the different estimates of vertical motion at the 5-m level instead of 12 m above the surface. No significant improvement in the relationships was found at 5 m compared to 12 m. The lack of improvement may be due to the frequent decrease of $\bar{w}$ closer to the surface, resulting in a smaller signal-to-noise ratio.

As a further sensitivity study, the direct method $\bar{w}$ estimates were recalculated at 12 m using the same procedures described above but only using nocturnal data. Despite this attempt to ''tune'' the tilt correction for nocturnal conditions, the relationship between the direct vertical motion estimates and those from mass continuity did not significantly improve for nocturnal periods.

5.2. Composite $\bar{w}$ estimates

The four different methods of obtaining $\bar{w}$ yield four different 3-month composite diurnal patterns (Fig. 10). The between-day variation (standard error in Fig. 10) of the mean $\bar{w}$ estimates is smaller for the mass continuity method compared to any of the direct methods. Contrary to the other methods tested, the Lee tilt correction approach leads to significant mean rising motion in the afternoon. This is related to the combination of a nonlinear dependence of $\bar{w}_m$ on wind speed and a strongly skewed wind speed distribution due to the high frequency of occurrence of weak winds.

The composited $\bar{w}$ from the direct methods and mass continuity disagree in sign during most of the night. Direct methods generally show rising motion of about 1 cm s^{-1} in contrast to weak sinking motion of 0.5 cm s^{-1} based on mass continuity (Fig. 10). The nocturnal sign difference could be due to the removal of the long-term mean sinking motion by the direct

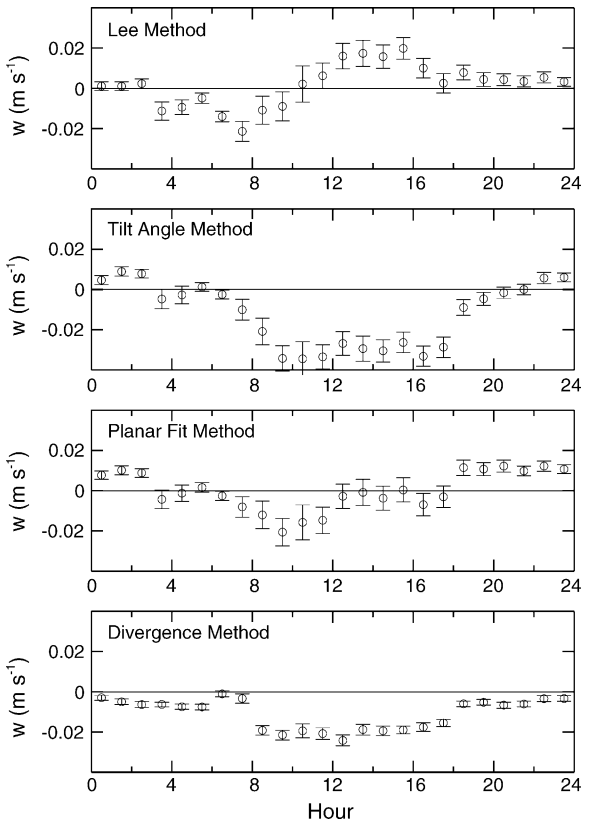

Fig. 10. Mean and standard error of the 3-month composite diurnal cycle of the 30-min mean vertical velocity from four different methods.

methods. As discussed above (Section 3), the direct methods fail at sites with non-zero long-term mean vertical motion.

6. NEE

In this section, composite nocturnal estimates of the individual terms in the conservation equation for NEE are contrasted. Following Staebler and Fitzjarrald (2004) and others, the expression for the net flux of CO_2 through a horizontal plane at height h is given by

$$\mathrm{NEE} = F_c + S_c + \int_0^h \bar{w}\frac{\partial \bar{c}}{\partial z}\,\mathrm{d}z + \int_0^h \bar{u}\frac{\partial \bar{c}}{\partial x}\,\mathrm{d}z \tag{7}$$

where F_c is the eddy-correlation flux and S_c is the storage term,

$$F_c \equiv (\bar{w}'\bar{c}')_h \tag{8}$$

$$S_c \equiv \int_0^h \frac{\partial \bar{c}}{\partial t}\,\mathrm{d}z \tag{9}$$

and where we have neglected the horizontal flux divergence term and simplified to two dimensions. The horizontal flux divergence is expected to be small (Staebler and Fitzjarrald, 2004; Mahrt and Vickers, 2005), although we are unaware of any direct measurements of this term for CO_2. This term may be significant at our site due to spatial heterogeneity. All terms on the rhs of Eq. (7), excluding horizontal advection (last term on rhs), were measured during the 3-month intensive field experiment. As an exercise, NEE is now estimated using a u_*-filter approach and the horizontal advection term will be estimated as a residual.

The storage term and the vertical gradient of CO_2 were measured at the central tower using a closed-path LICOR 6262 with inlets at 1, 5 and 12 m above ground. One-half hour records were used with centered time differencing. Vertical integration of the CO_2 tendency was performed using a piecewise linear function. The eddy-correlation flux was measured at 12 m using an open-path LICOR 7500 and a colocated Campbell CSAT3 sonic anemometer. The vertical advection term was evaluated following Lee (1998)

$$\int_0^h \bar{w}\frac{\partial \bar{c}}{\partial z}\,\mathrm{d}z \simeq \bar{w}_h\left(\bar{c}_h - h^{-1}\int_0^h \bar{c}\,\mathrm{d}z\right). \tag{10}$$

The composite nocturnal NEE is estimated with the following standard u_*-filter (Section 1) approach. As observed at many other sites, $(F_c + S_c)$ is small for weak mixing, increases with mixing strength and then approximately levels off (see below) in strong mixing conditions (Fig. 11). Because there is no reason for the NEE (respiration) to be dependent on the strength of the turbulence, the standard inference is that advective loss must be important in weak mixing periods. Conversely, for strong mixing conditions, the inference is that gradients, and therefore advection, are negligible within

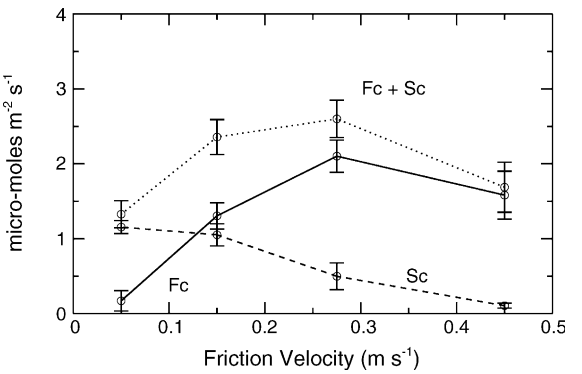

Fig. 11. Nocturnal eddy-correlation flux (F_c), storage (S_c) and their sum as a function of u_*. Standard error bars indicate night-to-night variability.

observational errors. We use the nights with stronger mixing to estimate the nocturnal NEE for the study period to be approximately 2.5 μ mol m^{-2} s^{-1}based on $(F_c + S_c)$ in high u_* conditions (Fig. 11). Our main conclusions are not sensitive to the precise value of NEE chosen.

We speculate that the decrease in nocturnal NEE for the highest u_* conditions (Fig. 11) is due to the u_*-dependence of the flux footprint. With weaker mixing, the footprint includes areas further upwind from the tower, while with stronger vertical mixing, the footprint shrinks. The decrease in NEE for the highest u_*cases implies that the respiration of CO_2 in the region of younger pines is smaller than in the surrounding area that has more mature trees, although we have no measurements of horizontal CO_2 gradients. Campbell et al. (2004) found that annual soil CO_2 effluxes in ponderosa pine stands 9–20 years old were 55% of those found in more mature stands. Interpretation is complicated due to spatial heterogeneity of the soil respiration even within the young pine site (Law et al., 2001).

Given an estimate for NEE, the horizontal advection term can be calculated as a residual using Eq. (7). The negative values for the horizontal advection term (Fig. 12) correspond to positive horizontal transport of relatively high CO_2 into the area from the surrounding forest. Such advection is consistent with higher respiration rates in the areas outside the study area.

The estimates in Fig. 12 indicate that the inferred horizontal and measured vertical advection terms are the largest terms in the budget for nights with weak mixing, and that they tend to cancel each other at this site. This possibility was predicted by Finnigan (1999), and observed by Aubinet et al. (2003), Feigenwinter et al. (2004) and Aubinet et al. (2005). That is, the net advection is the small difference between two large numbers of opposite sign. At this site, the sum of the horizontal and vertical advection terms is generally positive, corresponding to negative advection of relatively low CO_2 into the study area. The magnitude of the advection terms are within the range of those reported by Staebler and Fitzjarrald (2004) for the Harvard forest and Aubinet et al. (2005) for six different sites. Assuming that the estimate of $\bar{w}$ based on mass continuity is correct, and that long-term mean sinking motion due to the surface roughness change is realistic for this site, the vertical advection of CO_2 that would be calculated using the direct method nocturnal $\bar{w}$ would be of the wrong sign for most of the night regardless of the choice of tilt correction method.

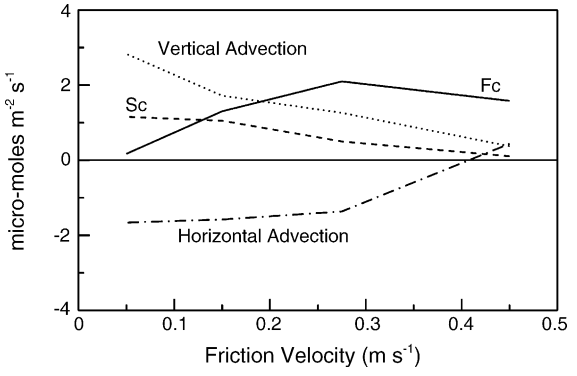

Fig. 12. Terms in the nocturnal NEE budget as a function of u_* (see text).

For nights with stronger mixing, the advection terms and the storage term are much smaller than the eddy-correlation flux. The strong mixing weakens the horizontal and vertical gradients of CO_2 and limits the accumulation (storage) of CO_2 near the ground. Despite stronger mean downward vertical velocity and stronger mean wind speed with increasing u_*, the advection terms become negligible compared to the eddy flux.

7. Conclusions

A 3-month field experiment was performed to contrast the mean vertical motion measured at a point on a central tower with the mean vertical motion calculated using mass continuity based on measurements from a network of towers surrounding the central tower. Three different tilt correction methods (direct methods) were applied. Typical values (mean absolute value of the 30-min mean $\bar{w}$) were 3–4 cm s^{-1} from the direct methods and 2 cm s^{-1} from mass continuity. The RMS difference in the 30-min average $\bar{w}$ estimates due to the choice of tilt correction method was 2–3 cm s^{-1}. In contrast to the mass continuity method, the tilt correction methods are sensitive to the time-scale chosen for averaging the wind components. The RMS differences between the 30-min average direct estimates of $\bar{w}$ and the estimates based on mass continuity were 4–5 cm s^{-1}. Of the three direct methods tested, $\bar{w}$ from the tilt angle method (as opposed to the regression based methods of Lee and the planar fit) most closely agreed with the $\bar{w}$ estimates based on mass continuity, but the disagreement is still large.

The hour-to-hour variations in $\bar{w}$ from the three direct methods are probably too large to be realistic or representative of the area. The estimate based on mass continuity is the most systematic and is consistent with subsidence due to the surface roughness change. For the site studied, $\bar{w}$ from mass continuity increases with the spatial scale over which the gradients of the mean wind

are calculated. The scale-dependence of the divergence at the site is thought to be related to the adjustment of the mean flow to an abrupt surface roughness change.

Mass continuity indicates long-term mean sinking motion for most times of day and night. Because the direct methods all remove the long-term mean $\bar{w}$, they fail to reproduce this result. Our conclusion is that more confidence can be attached to vertical motion estimates calculated from mass continuity, although such estimates could be sensitive to spatial scale. This result agrees with Heinesch et al. (2006), who recently concluded that mass continuity gives more realistic estimates of $\bar{w}$ compared to point measurements from a 3D anemometer.

Estimates of vertical advection of CO_2 based on mass continuity and the vertical CO_2 gradient indicate that it is the largest term in the NEE equation on weak mixing nights where strong vertical gradients of CO_2 coupled with weak systematic sinking motion transport lower CO_2 into the control volume. On strong mixing nights, the vertical advection is negligible due to weak vertical gradients despite stronger systematic sinking motion. We estimate that the nocturnal vertical and horizontal advection terms are of opposite sign and that they tend to cancel each other. In contrast to the mass continuity method, use of a tilt correction method to obtain $\bar{w}$ yields advection estimates that are not plausible.

Acknowledgments

We gratefully acknowledge the collection of the field data by John Wong and the helpful comments from the two reviewers. This research was supported by the NASA Terrestrial Ecology Program under Grant NAG5-11231 and by the Office of Science (BER), U.S. Department of Energy Grant DE-FG0203ER63653. The site is part of the AmeriFlux network.

References

Aubinet, M., Heinesch, B., Yernaux, M., 2003. Horizontal and vertical CO_2 advection in a sloping forest. Boundary-Layer Meteorol. 108, 397–417.

Aubinet, M., Berbigier, P., Bernhofer, C., Cescatti, A., Feigenwinter, C., Granier, A., Grunwald, T., Havrankova, K., Heinesch, B., Longdoz, B., Marcolla, B., Montagnani, L., Sedlak, P., 2005. Comparing CO_2 storage and advection conditions at night at different Carboneuroflux sites. Boundary-Layer Meteorol. 116, 63–94.

Baldocchi, D., Finnigan, J., Wilson, K., Paw U, K.T., Falge, E., 2000. On measuring net ecosystem carbon exchange over tall vegetation on complex terrain. Boundary-Layer Meteorol. 96, 257–291.

Berger, B.W., Davis, K.J., Yi, C., Bakwin, P.S., Zhao, C.L., 2001. Long-term carbon dioxide fluxes from a very tall tower in a northern forest: Flux measurement methodology. J. Atmos. Ocean. Technol. 18, 529–542.

Campbell, J.L., Sun, O.J., Law, B.E., 2004. Supply-side controls on soil respiration among Oregon forests. Glob. Change Biol. 10, 1857–1869.

Falge, E., Baldocchi, D., Olson, R., Anthoni, P., Aubinet, M., Bernhofer, C., Burba, G., Ceulemans, R., Clement, R., Dolman, H., Granier, A., Gross, P., Grunwald, T., Hollinger, D., Jensen, N.O., Katul, G., Keronen, P., Kowalski, A., Lai, C.T., Law, B.E., Meyers, T., Moncrieff, J., Moors, E., Munger, J.W., Pilegaard, K., Rannik, U., Rebmann, C., Suyker, A., Tenhunen, J., Tu, K., Verma, S., Vesala, T., Wilson, K., Wofsky, S., 2001. Gap-filling strategies for defensible annual sums of net ecosystem exchange. Agric. Forest Meteorol. 107, 43–69.

Feigenwinter, C., Bernhofer, C., Vogt, R., 2004. The influence of advection on the short-term CO_2 budget in and above a forest canopy. Boundary-Layer Meteorol. 113, 201–224.

Finnigan, J., 1999. A comment on the paper by Lee (1998): on micrometeorological observations of surface-air exchange over tall vegetation. Agric. Forest Meteorol. 97, 55–64.

Finnigan, J., Clement, P., Malhi, Y., Leuning, R., Cleugh, H.A., 2003. A re-evaluation of long-term flux measurement techniques. Part I: Averaging and coordinate rotation. Boundary-Layer Meteorol. 107, 1–48.

Garratt, J.R., 1990. The internal boundary layer – a review. Boundary-Layer Meteorol. 50, 171–203.

Goulden, M.L., Munger, J.W., Fan, S.-M., Daube, B.C., Wofsy, S.C., 1996. Measurements of carbon sequestration by long-term eddy covariance: methods and a critical evaluation of accuracy. Glob. Change Biol. 2, 169–182.

Heinesch, B., Yernauz, M., Aubinet, M., 2006. Some methodological questions concerning advection measurements: a case study. Boundary-Layer Meteorol., submitted for publication.

Högström, U., Smedman, A.-S., 2004. Accuracy of sonic anemometers: Laminar wind-tunnel calibrations compared to atmospheric in situ calibrations against a reference instrument. Boundary-Layer Meteorol. 111, 33–54.

Kaimal, J.C., Finnigan, J.J., 1994. Atmospheric Boundary Layer Flows. Oxford University Press, New York.

Law, B.E., Kelliher, F.M., Baldocchi, D.D., Anthoni, P.M., Irvine, J., 2001. Spatial and temporal variation in respiration in a young ponderosa pine forest during a summer drought. Agric. Forest Meteorol. 110, 27–43.

Lee, X., 1998. On micrometeorological observations of surface-air exchange over tall vegetation. Agric. Forest Meteorol. 91, 39–49.

Mahrt, L., Vickers, D., 2005. Boundary-layer adjustment over small-scale changes of surface heat flux. Boundary-Layer Meteorol. 116, 313–330.

Pattey, E., Strachan, I.B., Desjardins, R.L., Massheder, J., 2002. Measuring nighttime carbon dioxide flux over terrestrial ecosystems using eddy covariance and nocturnal boundary layer methods. Agric. Forest Meteorol. 113, 145–158.

Paw U, K.T., Baldocchi, D., Meyers, T.P., Wilson, K.B., 2000. Correction of eddy-covariance measurements incorporating both advective effects and density fluxes. Boundary-Layer Meteorol. 97, 487–511.

Staebler, R.M., Fitzjarrald, D.R., 2004. Observing subcanopy CO_2 advection. Agric. Forest Meteorol. 122, 139–156.

Vickers, D., Mahrt, L., 2003. The cospectral gap and turbulent flux calculations. J. Atmos. Ocean. Technol. 20, 660–672.

Wilczak, J.M., Oncley, S.P., Stage, S.A., 2001. Sonic anemometer tilt correction algorithms. Boundary-Layer Meteorol. 99, 127–150.